

SDiT: Spiking Diffusion Model with Transformer

Shu Yang , Hanzhi Ma , Member, IEEE, Chengting Yu , Aili Wang , Member, IEEE, Er-Ping Li , Fellow, IEEE

Abstract—Spiking neural networks (SNNs) have low power consumption and bio-interpretable characteristics, and are considered to have tremendous potential for energy-efficient computing. However, the exploration of SNNs on image generation tasks remains very limited, and a unified and effective structure for SNN-based generative models has yet to be proposed. In this paper, we explore a novel diffusion model architecture within spiking neural networks. We utilize transformer to replace the commonly used U-net structure in mainstream diffusion models. It can generate higher quality images with relatively lower computational cost and shorter sampling time. It aims to provide an empirical baseline for research of generative models based on SNNs. Experiments on MNIST, Fashion-MNIST, and CIFAR-10 datasets demonstrate that our work is highly competitive compared to existing SNN generative models.

Index Terms—Image generation, deep learning, spiking neural network

I. INTRODUCTION

SPIKING neural networks (SNNs) are considered to be the third generation of neural networks with higher biological interpretability, event-driven properties, and lower power consumption, and thus have the potential to become competitive alternatives to Artificial Neural Networks (ANNs) in the future. In SNNs, all information is encoded in spike sequences, enabling SNNs to perform accumulative operations at lower power budgets for energy efficiency.

SNNs trained with deep learning techniques, especially surrogate gradient learning methods [1], have shown promising results on basic tasks like image classification and segmentation [2]. However, the application of SNNs on more complex computer vision tasks, especially generative models, has been limited.

Recently, diffusion models have achieved significant success on image generation [3], owing to their robust training objectives derived from a likelihood perspective. They provide flexibility in model designs without constraints on their network architecture [4]. Some works [5][6] have attempted to use diffusion models with different backbones. In the field of SNN-based image generation, preliminary attempts like Spiking-GAN [7] and FSVAE [8] have been made but the results are not on par with ANNs. SDDPM [9] and SPIKING-DIFFUSION [10] attempt to introduce diffusion models into the SNNs.

This work was supported by the National Natural Science Foundation of China under Grant No.62071424 and 62027805, and National Key Research and Development Program of China under Grant No.2023YFB3812500. (Corresponding authors: Hanzhi Ma; Er-Ping Li.)

Shu Yang, Hanzhi Ma, Chengting Yu, Aili Wang, Er-Ping Li are with ZJU-UIUC Institute, Zhejiang University, Haining, Zhejiang 314400, China (e-mail: shu.23@intl.zju.edu.cn; mahanzhi@zju.edu.cn; chengting.21@intl.zju.edu.cn; ailiwang@intl.zju.edu.cn; liep@zju.edu.cn).

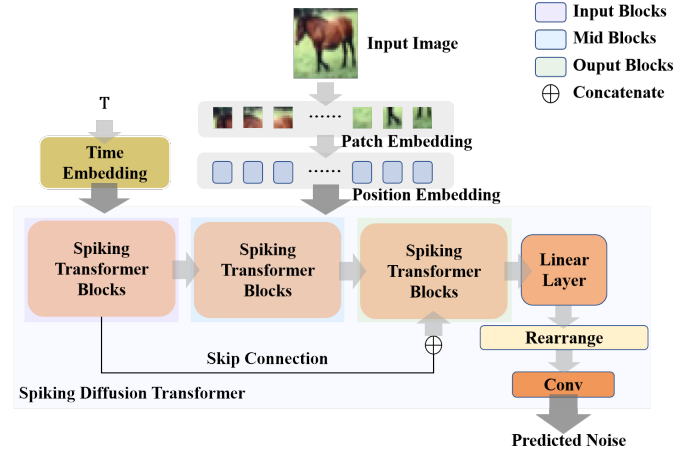


Fig. 1. Diagram of SDiT architecture, illustrating the flow from input time and patch embeddings through multiple spiking transformer blocks with skip connections, culminating in a final processing stage with linear and convolutional layers for predicted noise generation.

In this work, we propose Spiking Diffusion Transformer (SDiT), a novel SNN diffusion model architecture based on transformer. It demonstrates superior image generation potential for SNNs. We employ an efficient self-attention : RWKV[11], and introduce the Reconstruction Module, a specially designed module aimed at supplementing information lost after the firing of spiking neurons, thereby enhancing the quality of the reconstructed image. Comprehensive experiments on MNIST [12], Fashion-MNIST [13] and CIFAR-10 [14] show that SDiT has great competitiveness among the existing image generation models based on SNNs.

II. PRELIMINARY

RWKV [11] is a powerful competitor to the self-attention mechanism in transformer that can achieve efficient self-attention under low computational complexity.

Given an input vector X at position t , first apply linear transformations $r_t = XW_r$, $k_t = XW_k$, $v_t = XW_v$, where W_r , W_k , W_v are linear transformation matrices. X is obtained by weighting the original input and input from the previous timestep, referred to as token-shift. r_t is referred to as the reception matrix with each element indicating the reception of past information. K and V are analogous to the key and value matrices in self-attention.

The attention output of RWKV is:

$$wkv_t = \frac{\sum_{i=1}^{t-1} e^{-(t-1-i)w+k_i} \odot v_i + e^{u+k_t} \odot v_t}{\sum_{i=1}^{t-1} e^{-(t-1-i)w+k_i} \odot v_i} \quad (1)$$

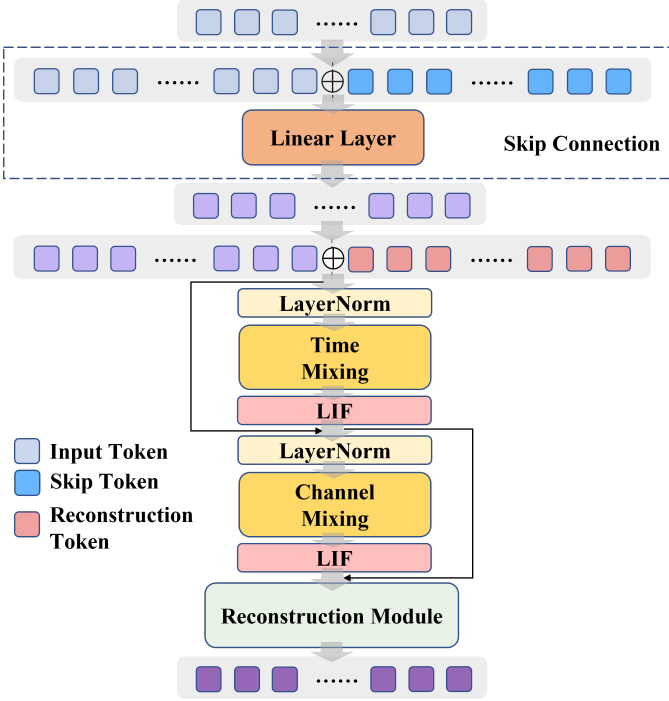


Fig. 2. Spiking Transformer Block. This block comprises skip connections from the previous block, Time-Mixing, LIF neurons, Channel-Mixing, and internal residual connections. Its core structure is analogous to that of a transformer block, with the key distinction being the substitution of self-attention by RWKV. The Reconstruction Module disassembles the previously concatenated Reconstruction Tokens, supplementing the original vector with transformed information that includes the intrinsic dynamics of LIF neurons. This process compensates for the information loss in the original vector after it has been processed by spiking neurons.

where k_t is the vector of row i in k_t , v_t is the vector of row i in v_t , \odot is the Hadamard product, w is a learnable position weight decay vector, and u prevents the degeneration of w .

Time-Mixing is defined on top of the RWKV attention output by adding a linear output layer:

$$o_t = W_o(\sigma(r_t) \odot wkv_t) \quad (2)$$

Channel-Mixing is defined as:

$$o_t = \sigma(r_t) \odot (W_v \max(k_t, 0)^2) \quad (3)$$

where W_o and W_v are linear transformations, σ is the Sigmoid function applied to r_t . By applying Sigmoid to r_t , unnecessary historical information is eliminated, serving as a “forget gate” to obtain the output.

Time-Mixing can be simply seen as a replacement for standard self-attention, and Channel-Mixing as a replacement for the Feed-Forward Network (FFN) layer.

III. PROPOSED METHOD

A. Overview of SDiT Architecture

Due to the distinct neuronal mechanisms in SNNs compared to ANNs, the integration of complex self-attention mechanisms, which add to the model’s parameter count, often leads to training difficulties, even when using gradient approximation techniques. To facilitate more efficient training, we

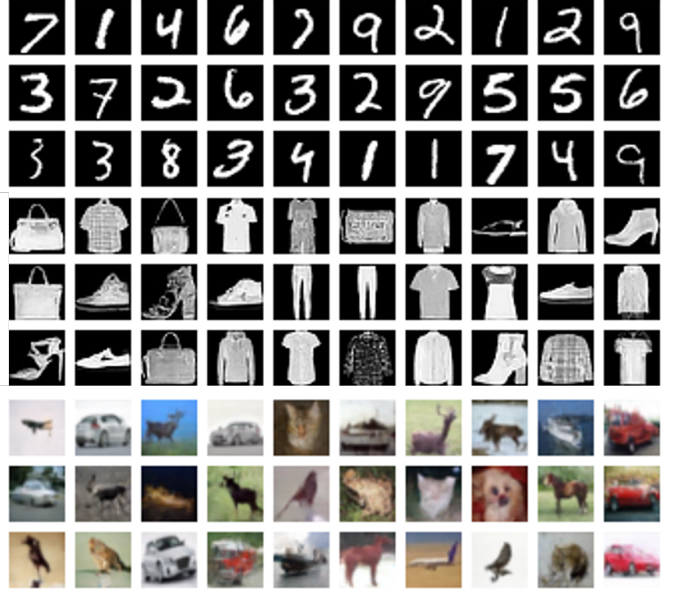


Fig. 3. Samples on different datasets. The first three rows from the top represent MNIST, the middle three rows depict Fashion-MNIST, and the final three rows correspond to CIFAR-10.



Fig. 4. Samples on MNIST without Reconstruction Module.

propose incorporating the RWKV mechanism, known for its approximate linear computational complexity, into SNNs. This approach, inspired by the Attention Free Transformer [15], simplifies the model by reducing both computational and parameter complexity. RWKV, offering performance comparable to traditional self-attention, is utilized as a more efficient alternative in our transformer model.

Fig. 1 shows the overview of the network architecture. Before entering the model, the input image first goes through patch embedding, which is then goes through position embedding. The denoising timestep goes through time embedding before entering the model. Inspired by the U-ViT [6], the model consists of three stages of Spiking Transformer Blocks. The Input Blocks serve as the first stage of the input processing, where each block outputs are directed into two separate paths - one that connects directly to the next block, and the other that forms skip connections to the corresponding blocks in the Output Blocks. The outputs from the Spiking Transformer Blocks are then fed into the Final Layer to be mapped back to the original image size. Following patch reconstruction and a convolution layer, the final predicted noise is obtained.

B. Embedding

Before inputting into the Spiking Diffusion Transformer, embedding operations are first performed on the image and denoising timestep.

As shown in Fig. 1, the denoising timestep is embedded into the same dimensional space as the position embeddings. For the image, it is first divided into patches and mapped to a high dimensional space through patch embedding. Finally, position embedding is applied to supplement positional information for each token.

C. Spiking Transformer Block

The structure of the Spiking Transformer Block is shown in Fig. 2.

Given an input vector $x \in \mathbb{R}^{B \times N \times D}$, where B is the batch size, N is the sequence length of patches, and D is the feature dimension.

Let \mathcal{F} denote the function for processing skip connections:

$$x = \mathcal{F}(x, x_{skip}) \quad (4)$$

$$\mathcal{F}(x, x_{skip}) = \begin{cases} ([x; x_{skip}])W_{skip}, & \text{if } x_{skip} \text{ not } None \\ x & \end{cases} \quad (5)$$

where $[\cdot]$ denotes concatenation, and $W_{skip} \in \mathbb{R}^{2D \times D}$ is a linear transformation. For Input Blocks and Mid Blocks, x_{skip} is *None*; for Output Blocks, x_{skip} is the output from the corresponding Input Block.

Introduce a Reconstruction Token denoted as $z \in \mathbb{R}^{1 \times N \times D}$, and tiled before being concatenated to x :

$$\hat{x} = [x; z \otimes \mathbf{1}_B] \in \mathbb{R}^{B \times 2N \times D} \quad (6)$$

where \otimes denotes the Kronecker product, and $\mathbf{1}_B$ is an all-ones vector.

The concatenated \hat{x} is then fed into the Time-Mixing and Channel-Mixing modules. After passing through Leaky Integrate-and-Fire (LIF) neurons, residual connections are added:

$$x_{Attn} = \hat{x} + LIF(TimeMixing(LN(\hat{x}))) \quad (7)$$

$$x_{FFN} = x_{Attn} + LIF(ChannelMixing(LN(x_{Attn}))) \quad (8)$$

where LN denotes *LayerNorm* [16].

Finally, the Channel-Mixing output is processed:

$$y = \mathcal{G}(x_{FFN}) \quad (9)$$

where \mathcal{G} denotes operations on the Reconstruction Module.

D. Reconstruction Module

Time-Mixing is a unique self-attention mechanism. Directly applying standard self-attention spaces with complex representations to the spiking representations in SNNs leads to significant information loss when the outputs are input into spiking neurons.

To compensate for this, we designed the Reconstruction Token and Reconstruction Module. The Reconstruction Token is comprised of learnable parameters. After embedding the Reconstruction Token, it can represent the intrinsic dynamic

TABLE I
RESULTS ON DIFFERENT DATASETS.

Dataset	Model	Time Steps	FID	IS
MNIST	SGAD	16	69.64	-
	FSVAE	16	97.06	6.209
	Spiking-Diffusion	16	37.50	-
	SDDPM	4	29.48	-
	SDiT	4	5.54	2.452
Fashion-MNIST	SGAD	16	165.42	-
	FSVAE	16	90.12	4.551
	Spiking-Diffusion	16	91.98	-
	SDDPM	4	21.38	-
	SDiT	4	5.49	4.549
CIFAR-10	SGAD	16	181.50	-
	FSVAE	16	175.50	2.945
	Spiking-Diffusion	16	120.50	-
	SDDPM	4	16.89	7.655
	SDiT	4	22.17	4.080

TABLE II
ABLATION EXPERIMENTS EVALUATING FID ON DIFFERENT DATASETS.

Model	Reconstruction Module	MNIST	Fashion-MNIST
SDiT	✗	224.66	111.52
SDiT	✓	5.54	5.49

information of spiking neurons. In the Reconstruction Module, the original outputs are rescaled to mitigate the information loss when passed through spiking neurons. The effectiveness of this is shown in Section IV.

After computations over the concatenated vector, the embedded Reconstruction Token is separated from the output vector.

$$y', z' = \text{split}(x_{FFN}) \quad (10)$$

where $y' \in \mathbb{R}^{B \times N \times D}$, $z' \in \mathbb{R}^{B \times N \times D}$, and split denotes the vector separation operation.

Since the Reconstruction Token has the same dimensions as the input, its feature dimension is first linearly transformed to match the number of patches:

$$z'_D = z'W_D \in \mathbb{R}^{B \times N \times N} \quad (11)$$

where $W_D \in \mathbb{R}^{D \times N}$, transforming along the second dimension.

Swapping the patch and feature dimensions, the patch dimension is then linearly transformed again to match the feature dimension:

$$z'_N = z'_D W_N \in \mathbb{R}^{B \times N \times D} \quad (12)$$

where $W_N \in \mathbb{R}^{N \times D}$, transforming along the second dimension.

Finally, the obtained vector is element-wise multiplied with the separated vector and added to it as supplementary information:

$$y = y' + z'_N \odot y' \quad (13)$$

where \odot denotes the Hadamard product.

TABLE III
NUMBER OF PARAMETERS AND MAC OPERATIONS.

Model	Backbone	Parameters	MACs
DiT	Transformer	13.86 M	3.48 G
SDiT	RWKV	11.67 M	1.32 G

E. Final Layer

The main function of this layer is to convert the output to a reconstructed image. After the Spiking Transformer Blocks, a linear transformation along the feature dimension is applied to match the original image size. Afterwards, the patches are reconstructed back into the image. Finally, a 3×3 convolutional block is applied based on [6], which can enhance the quality of generated samples.

IV. EXPERIMENT

A. Experiment Settings

1) *Evaluation Metrics*: We use Fréchet Inception Distance (FID) [17] to assess the quality of sampled images and Inception Score (IS) [18] to evaluate sample diversity. When computing FID, 50,000 images are sampled from the dataset and 50,000 images are generated to calculate FID between them. When computing the IS for MNIST and Fashion-MNIST datasets, the quantitative comparisons of IS to scores on ImageNet hold limited meaningfulness, owing to the substantial domain discrepancy between these data distributions versus ImageNet on which IS was originally proposed and validated.

2) *Implementation details*: We standardized the input size to 28×28 for both MNIST, Fashion-MNIST, and resized CIFAR-10 images for uniformity. The architecture for MNIST and Fashion-MNIST involves 2 Input and Output Blocks, 1 Mid Block, and a hidden dimension of 384. For CIFAR-10, this extends to 4 Input and Output Blocks, 1 Mid Block, and a 512 hidden dimension. Optimization is performed using AdamW with a learning rate of 1e-4, training MNIST and Fashion-MNIST models for 1600 epochs, and CIFAR-10 for 2000 epochs post-resizing. Our SNN models are developed using the SpikingJelly framework [19]. Experiments were conducted on 4xNVIDIA 4090 GPUs.

B. Comparisons

As depicted in Table I, our SDiT outperforms SGAD, FSVAE, Spiking-Diffusion and SDDPM on image reconstruction and generation on MNIST and Fashion-MNIST datasets. On CIFAR-10, the FID score of our SDiT is slightly higher than SDDPM but substantially lower than other methods, exhibiting strong image generation capabilities. Fig. 3 shows example of generated images from our method on the three datasets. It can be observed that under very short spiking time steps, our approach can synthesize sharper images with more defined edges.

C. Ablation Study

If the transformer structure is directly introduced into SNNs without adaptation, there would be immense information loss

compared to the sparse spiking signals emitted by SNN neurons. To address this problem, we designed the Reconstruction Module to align both.

As shown in Table II, models without the Reconstruction Module have very high FID scores on MNIST and Fashion-MNIST datasets. The generated image quality is also poor, with blurred edges and noise dominating the scene, as shown in Fig. 4. In contrast, our model with the Reconstruction Module encodes the intrinsic dynamics of SNN neurons through the evolution of Reconstruction Tokens in the data flow. This leads to significantly better performance.

Additionally, our method employs RWKV as an alternative self-attention which effectively integrates with SNNs. When configured with the same model settings, as depicted in Table III, our approach attains a smaller parameter size and lower multiply-accumulates (MACs) compared to the pure transformer ANN implementation (DiT) [5], thus fully demonstrating the low-power advantage of SNNs.

V. DISCUSSION

Despite the relatively strong performance, SDiT has some limitations. The performance of SDiT on MNIST and Fashion-MNIST significantly surpasses other methods. However, on CIFAR-10, its results fail to reach state-of-the-art levels. We attribute this underperformance, to some extent, to the inferior efficacy of Vision transformers when trained on limited data. While images in MNIST and Fashion-MNIST encode relatively simple visual information, the intrinsic complexity and comparatively low resolution of CIFAR-10 images obscures fine-grained edge details in SDiT's learned representations. Regarding the integration of self-attention mechanisms and SNNs, we plan to incorporate more fine-grained schemes in future work to further minimize the information loss of self-attention within the SNN framework.

Another limitation is that the embedding component of SDiT is not implemented with a pure SNN. The current SDiT consists of a hybrid architecture of ANN and SNN. As image sizes scale up, the parameter and computation amounts in the ANN module also increase, which may diminish the inherent low-power characteristics of SNNs due to parameter growth in the portion of ANN. In future work, our plan is to explore designs fully contained within the SNN framework and attempt to construct models with a pure SNN architecture.

VI. CONCLUSION

In this work, we propose a novel generative spiking neural network architecture : SDiT, which combines the low power consumption property of SNNs with superior generative capabilities. As a new effort that incorporates transformer as the backbone for diffusion models in the SNN domain, SDiT has advanced the state-of-the-art in terms of generated image quality and exhibits strong performance across multiple datasets. We envision that this research can introduce new perspectives to the field of SNN generative model for future developments in this area.

REFERENCES

[1] E. O. Neftci, H. Mostafa, and F. Zenke, “Surrogate gradient learning in spiking neural networks: Bringing the power of gradient-based optimization to spiking neural networks,” *IEEE Signal Processing Magazine*, vol. 36, no. 6, pp. 51–63, 2019.

[2] J. D. Nunes, M. Carvalho, D. Carneiro, and J. S. Cardoso, “Spiking neural networks: A survey,” *IEEE Access*, vol. 10, pp. 60738–60764, 2022.

[3] P. Dhariwal and A. Nichol, “Diffusion models beat gans on image synthesis,” *Advances in neural information processing systems*, vol. 34, pp. 8780–8794, 2021.

[4] R. Rombach, A. Blattmann, D. Lorenz, P. Esser, and B. Ommer, “High-resolution image synthesis with latent diffusion models,” in *Proceedings of the IEEE/CVF conference on computer vision and pattern recognition*, pp. 10684–10695, 2022.

[5] W. Peebles and S. Xie, “Scalable diffusion models with transformers,” in *Proceedings of the IEEE/CVF International Conference on Computer Vision*, pp. 4195–4205, 2023.

[6] F. Bao, S. Nie, K. Xue, Y. Cao, C. Li, H. Su, and J. Zhu, “All are worth words: A vit backbone for diffusion models,” in *Proceedings of the IEEE/CVF Conference on Computer Vision and Pattern Recognition*, pp. 22669–22679, 2023.

[7] V. Kotariya and U. Ganguly, “Spiking-gan: A spiking generative adversarial network using time-to-first-spike coding,” in *2022 International Joint Conference on Neural Networks (IJCNN)*, pp. 1–7, 2022.

[8] H. Kamata, Y. Mukuta, and T. Harada, “Fully spiking variational autoencoder,” in *Proceedings of the AAAI Conference on Artificial Intelligence*, vol. 36, pp. 7059–7067, 2022.

[9] J. Cao, Z. Wang, H. Guo, H. Cheng, Q. Zhang, and R. Xu, “Spiking denoising diffusion probabilistic models,” in *Proceedings of the IEEE/CVF Winter Conference on Applications of Computer Vision*, pp. 4912–4921, 2024.

[10] M. Liu, R. Wen, and H. Chen, “Spiking-diffusion: Vector quantized discrete diffusion model with spiking neural networks,” *arXiv preprint arXiv:2308.10187*, 2023.

[11] B. Peng, E. Alcaide, Q. Anthony, A. Albalak, S. Arcadinho, H. Cao, X. Cheng, M. Chung, M. Grella, K. K. GV, *et al.*, “Rwkv: Reinventing rnns for the transformer era,” *arXiv preprint arXiv:2305.13048*, 2023.

[12] Y. LeCun, C. Cortes, C. Burges, *et al.*, “Mnist handwritten digit database,” 2010.

[13] H. Xiao, K. Rasul, and R. Vollgraf, “Fashion-mnist: a novel image dataset for benchmarking machine learning algorithms,” *arXiv preprint arXiv:1708.07747*, 2017.

[14] A. Krizhevsky, G. Hinton, *et al.*, “Learning multiple layers of features from tiny images,” 2009.

[15] S. Zhai, W. Talbott, N. Srivastava, C. Huang, H. Goh, R. Zhang, and J. Susskind, “An attention free transformer,” *arXiv preprint arXiv:2105.14103*, 2021.

[16] J. L. Ba, J. R. Kiros, and G. E. Hinton, “Layer normalization,” *arXiv preprint arXiv:1607.06450*, 2016.

[17] M. Heusel, H. Ramsauer, T. Unterthiner, B. Nessler, and S. Hochreiter, “Gans trained by a two time-scale update rule converge to a local nash equilibrium,” *Advances in neural information processing systems*, vol. 30, 2017.

[18] T. Salimans, I. Goodfellow, W. Zaremba, V. Cheung, A. Radford, and X. Chen, “Improved techniques for training gans,” *Advances in neural information processing systems*, vol. 29, 2016.

[19] W. Fang, Y. Chen, J. Ding, Z. Yu, T. Masquelier, D. Chen, L. Huang, H. Zhou, G. Li, and Y. Tian, “Spikingjelly: An open-source machine learning infrastructure platform for spike-based intelligence,” *Science Advances*, vol. 9, no. 40, p. eadi1480, 2023.

[20] H. Cao, C. Tan, Z. Gao, Y. Xu, G. Chen, P.-A. Heng, and S. Z. Li, “A survey on generative diffusion model,” *arXiv preprint arXiv:2209.02646*, 2022.

[21] L. Feng, D. Zhao, and Y. Zeng, “Sgad: Spiking generative adversarial network with attention scoring decoding,” *arXiv preprint arXiv:2305.10246*, 2023.

[22] J. Ho, A. Jain, and P. Abbeel, “Denoising diffusion probabilistic models,” *Advances in neural information processing systems*, vol. 33, pp. 6840–6851, 2020.

[23] W. Maass, “Networks of spiking neurons: the third generation of neural network models,” *Neural networks*, vol. 10, no. 9, pp. 1659–1671, 1997.

[24] Y. Song and S. Ermon, “Generative modeling by estimating gradients of the data distribution,” *Advances in neural information processing systems*, vol. 32, 2019.

[25] Y. Song, J. Sohl-Dickstein, D. P. Kingma, A. Kumar, S. Ermon, and B. Poole, “Score-based generative modeling through stochastic differential equations,” *arXiv preprint arXiv:2011.13456*, 2020.

[26] A. Vaswani, N. Shazeer, N. Parmar, J. Uszkoreit, L. Jones, A. N. Gomez, Ł. Kaiser, and I. Polosukhin, “Attention is all you need,” *Advances in neural information processing systems*, vol. 30, 2017.

[27] A. Dosovitskiy, L. Beyer, A. Kolesnikov, D. Weissenborn, X. Zhai, T. Unterthiner, M. Dehghani, M. Minderer, G. Heigold, S. Gelly, *et al.*, “An image is worth 16x16 words: Transformers for image recognition at scale,” *arXiv preprint arXiv:2010.11929*, 2020.

[28] H. Zheng, Y. Wu, L. Deng, Y. Hu, and G. Li, “Going deeper with directly-trained larger spiking neural networks,” in *Proceedings of the AAAI conference on artificial intelligence*, vol. 35, pp. 11062–11070, 2021.

[29] W. Fang, Z. Yu, Y. Chen, T. Huang, T. Masquelier, and Y. Tian, “Deep residual learning in spiking neural networks,” *Advances in Neural Information Processing Systems*, vol. 34, pp. 21056–21069, 2021.

[30] Y. Hu, L. Deng, Y. Wu, M. Yao, and G. Li, “Advancing spiking neural networks towards deep residual learning,” *arXiv preprint arXiv:2112.08954*, 2021.

[31] Q. Su, Y. Chou, Y. Hu, J. Li, S. Mei, Z. Zhang, and G. Li, “Deep directly-trained spiking neural networks for object detection,” in *Proceedings of the IEEE/CVF International Conference on Computer Vision*, pp. 6555–6565, 2023.

[32] Z. Zhou, Y. Zhu, C. He, Y. Wang, S. Yan, Y. Tian, and L. Yuan, “Spikformer: When spiking neural network meets transformer,” *arXiv preprint arXiv:2209.15425*, 2022.

[33] R.-J. Zhu, Q. Zhao, and J. K. Eshraghian, “Spikegpt: Generative pre-trained language model with spiking neural networks,” *arXiv preprint arXiv:2302.13939*, 2023.

[34] D. P. Kingma and M. Welling, “Auto-encoding variational bayes,” *arXiv preprint arXiv:1312.6114*, 2013.

[35] O. Ronneberger, P. Fischer, and T. Brox, “U-net: Convolutional networks for biomedical image segmentation,” in *Medical Image Computing and Computer-Assisted Intervention–MICCAI 2015: 18th International Conference, Munich, Germany, October 5–9, 2015, Proceedings, Part III* 18, pp. 234–241, Springer, 2015.

[36] J. Song, C. Meng, and S. Ermon, “Denoising diffusion implicit models,” *arXiv preprint arXiv:2010.02502*, 2020.

[37] A. Q. Nichol and P. Dhariwal, “Improved denoising diffusion probabilistic models,” in *International Conference on Machine Learning*, pp. 8162–8171, PMLR, 2021.

[38] A. Van Den Oord, O. Vinyals, *et al.*, “Neural discrete representation learning,” *Advances in neural information processing systems*, vol. 30, 2017.